Wideband Microstrip Antenna Integrated With Optimized Buffer Layer Parameters For Underwater Wireless Communication

Hanisah Mohd Zali, Idnin Pasya Ibrahim, Mohd Tarmizi Ali and Mohd Khairil Azhar Mahmood

***Abstract*— Transmitting electromagnetic waves in underwater environment is a challenge, due to the lossy properties of water. Using conventional antennas for transmission in these environments results in severe signal attenuation, partly attributed to un-optimized antenna parameters. In this paper, a conventional wideband circular patch antenna integrated with an optimized buffer layer structure was proposed for underwater applications. From simulation, the optimized buffer materials and sizes shows improvements in antenna performance while operating underwater within a wide frequency range. The antenna with the optimized buffer layer was fabricated and measured in a laboratory water tank for verification. The measurement results agree well with the simulated results, verifying the effectiveness of the utilization of an optimized buffer layer in underwater environment.**

***Index Terms*— Underwater Antennas; wide frequency band; buffer layer structure; return loss.**

I. INTRODUCTION

UNDERWATER wireless communication and sensing nowadays become popular a research area due to its ability in supporting various underwater applications. This includes deep water search and rescue missions, seabed and subsurface sensing and wireless networks among sensor nodes, divers as well as underwater robots and autonomous vehicles.

In underwater applications, wireless communication and sensing systems using acoustic technology is widely used. Nevertheless, they have several drawback such as narrow bandwidth and susceptibility to propagation characteristics from background media [1], rendering them less suitable for high speed data transmission. Hence, for such applications, the usage of electromagnetic waves is preferable, particularly in implementation of high data rate wireless underwater communication due to wider bandwidth, and increased data capacity [2, 3].

This manuscript is submitted on 17th February 2019 and accepted on 12th July 2019. This research work is partly supported by Exploratory Research Grant Scheme under the Ministry of Higher Education of Malaysia, Grant number FRGS/1/2015/TK04/UITM/02/32. Hanisah Mohd Zali, Idnin Pasya Ibrahim, Mohd Tarmizi Ali and Mohd Khairil Azhar Mahmood are from Faculty of Electrical Engineering, Universiti Teknologi MARA, Shah Alam, 40450 Selangor, Malaysia. (email:mohdkhairiladzhar@gmail.com).

However, underwater electromagnetic wave transmission suffers from high transmission loss, severe multipath fading and propagation delay, especially at high frequencies. In literature, several research on underwater wireless communication were reported covering topics on propagation characteristics [4, 5], as well as techniques and transmission schemes for MHz and GHz frequency regions [6, 7]. These reports indicated the issue of poor signal-to-noise ratio, which can only be improved by using enhanced underwater antenna design.

There are several reports on designing underwater antennas. Most of them proposed insulated antennas [8], and others presented antenna covered by containers while operating underwater. For example, the researcher in [9] and [10] uses a container filled with tap water as the insulation of the antenna operating underwater. However, the utilization of non-optimized containers as the antenna is limiting the antenna performance underwater due to impedance mismatch. To the author's knowledge, the relationship between antenna insulator parameters and antenna performance has not been fully studied.

Meanwhile, Ngunyen et al. investigated similar antenna structure using insulator for antennas implanted inside human body [11], showing that the antenna efficiency can be improved by changing the parameters of the insulator itself. Taking similar initiative, the authors of this present paper investigated an underwater antenna structure using container with optimized parameters (afterwards termed "buffer layer") to improve antenna performance when operating underwater.

In this paper, a wideband underwater antenna design using a circular patch topology integrated with an optimized buffer layer structure is presented. A conventional circular patch antenna with half ground plane was selected as a base antenna to accommodate a wide signal bandwidth. The buffer layer structure was designed using liquid materials with a specific permittivity value and size. The antenna performance was observed in term of return loss (S_{11}), gain and efficiency, while changing the parameters of the buffer layer.

It will be shown through simulations and experiments that in underwater environments (this paper mainly addresses freshwater), the proposed antenna resulted an improvements in return loss and bandwidth when using a buffer materials with permittivity value calculated by geometric average calculation and the buffer size is equals to the nearfield region of the antenna.

The organization of this paper will start with the base antenna design, followed by the parametric study on buffer layer structure. The effects on the performance of the simulated proposed antenna was analysed and presentend in section III. Section IV presented the measured results using a fabricated antenna structure and the experimental setup conducted in laboratory water tank was discussed.

II. ANTENNA DESIGN STRUCTURE

A. *Structure of Base Antenna Designs*

In this design, the antenna was simulated using CST Microwave Studio software. Firstly, The antenna was design to operate within a wide frequency bandwidth to accomodate high data rate transmission. Half ground plane technique was uses in order to develop a wide frequency band. The antenna parameters was design using circular patch topology, similar approaches by [12]. The radius of the patch was determined by

$$a = \frac{F}{\left\{1+\frac{2hp}{\pi\varepsilon_r F}\left[\ln\left(\frac{\pi F}{2h}+1.77216\right)\right]\right\}^{1/2}} \quad (1)$$

where

$$F = \frac{8.791\times10^{9}}{f_r\sqrt{\varepsilon_r}} \quad (2)$$

hp is the thickness of the patch (copper),ε_r is the substrate dielectric constant (FR-4), and f_r is the resonant frequency. A partial ground plane was used for return loss and bandwidth improvement [13].

The dimension of base antenna design was fabricated using same dimension parameter as in simulation design. Figures 1(a), 1(b) shows the geometry of the basic wideband antenna design and Figure 1(c) show the fabricated antenna. Table I shows the final parameters dimension of the base antenna. The dimension of the base antenna parameters such as the radiating patch, feedline and ground plane were optimized to get the optimum result and the final dimension was presented in Table 1.

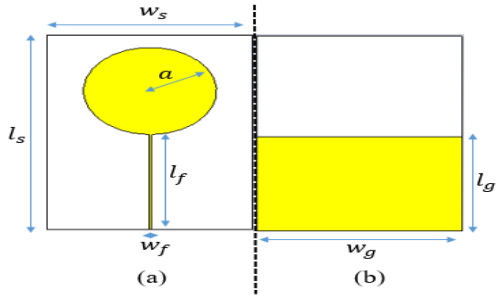

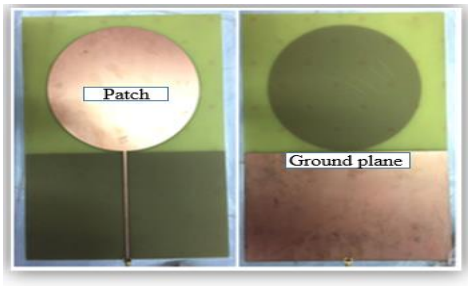

(c)

Fig.1. Base antenna design: 1(a) Front View , 1(b) Back View ,1(c) Fabricated antenna

TABLE I
DIMENSION OF THE BASE ANTENNA

Parameter	Symbol	Dimension (mm)
Radius patch	a	65
Width feedline	w_f	2.95
Length feedline	l_f	147.5
Width Ground	w_g	200
Length Ground	l_g	140
Width Substrate	w_s	200
Length Substrate	l_s	290
Thickness Substrate	t_s	1.6

B. *Integration of Base Antenna with Buffer Layer Design*

Secondly, the base antenna was inserted within a buffer layer structure. Besides functioning as a container for the antenna, the proposed buffer layer also acts as a matching layer between the antenna and the water surrounding it. The parameter of buffer layer was optimized in term of the relative permittivity (ε_{rb}) and the buffer size. This study proposes ε_{rb}, using geometric average calculation between air and water, shown by

$$\varepsilon_{rb} = \sqrt[k]{\varepsilon_{r1}\cdot\varepsilon_{r2}\cdot\varepsilon_{rk}} \quad (3)$$

where k is the number of medium to be considered.

To emulate an underwater environment, the parameters of simulation background were set to approximate freshwater water properties, resulting in ε_{rb} of 8.85. Other parameters were similar to a freshwater water. The buffer layer size was calculated based on the equation of reactive near field region which was using a buffer wavelength as shown in Equation (4) and (5).

$$R < 0.62\sqrt{\frac{D^3}{\lambda_b}} \quad (4)$$

$$\lambda_b = \frac{\lambda_\circ}{\left[\varepsilon_{r^2} + \left(\frac{\sigma}{\omega \cdot \varepsilon_\circ}\right)^2\right]^{1/4}} \quad (5)$$

where

$$\lambda_\circ = \frac{c}{f}, \omega = 2\pi f$$

R is the boundary of near field region, D is the maximum linear dimension of the antenna, λ_b is antenna wavelength in buffer, λ_o is antenna wavelength in free space, $\boldsymbol{\varepsilon}_r$ is relative permittivity, $\boldsymbol{\varepsilon}_o$ is relative permittivity in free space and $\boldsymbol{\sigma}$ is conductivity of background medium and c is a speed of light (3×10^8). The size of buffer layer was optimized in several different field region condition which leads to the difference in the buffer thickness, h. The Optimization was observed between Reactive Nearfield region conditions (h1), Radiative Nearfied (h2), Transmission line Theory (h3) and Reactive Nearfield Buffer (h4).Table II presented the equations of each regions conditions and the buffer thickness dimensions.

TABLE II
DIMENSION OF THE BUFFER LAYER THICKNESS AND THE RELATED EQUATION

Thickness	Calculation Basis	Equations	Dimension (mm)
h_1	Radiating Nearfield with water Refractive Index	$R \le \frac{2D^2}{\lambda}$, $\lambda = \frac{c/n}{f}$ n = refractive index of tap water	128
h_2	Reactive Nearfield	$R < 0.62\sqrt{\frac{D^3}{\lambda}}$, $\lambda = \frac{c/n}{f}$ n = refractive index of tap water	59.3
h_3	Transmission Line	$h_3 = \frac{\lambda}{4}$, $\lambda = \frac{c}{f}$	62.95
h_4	Reactive Nearfield Buffer (proposed size)	$R < 0.62\sqrt{\frac{D^3}{\lambda_b}}$ $\lambda_b = \frac{\lambda_\circ}{\left[\varepsilon_{r^2} + \left(\frac{\sigma}{\omega \cdot \varepsilon_\circ}\right)^2\right]^{1/4}}$	102.33

The base antenna integrated with buffer layer structure was fabricated using same dimension as in simulation. The buffer structure was fabricated using transparent acrylic glass material which is 6mm thickness. Figure 2 shows the geometry of the buffer layer structure and Table III presented the dimension of the buffer.

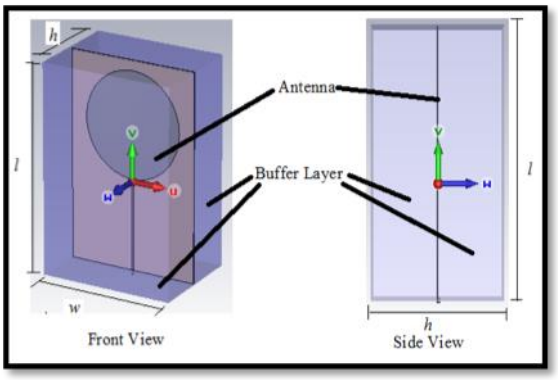

(a)

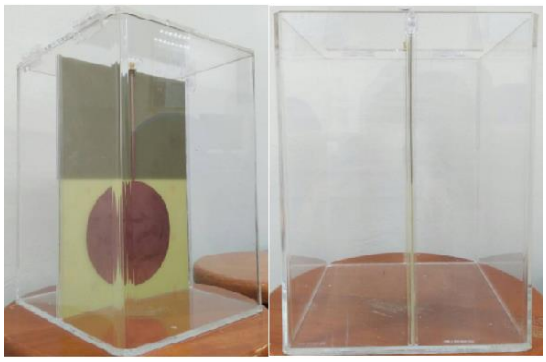

(b)

Fig.2. Base Antenna Design integrated with Buffer Layer Structure: 1(a) Simulated antenna and (b) Fabricated antenna

TABLE III
DIMENSION OF THE BUFFER STRUCTURE

Parameter		Dimension (mm)
Buffer Layer	Width , w	200
	Length , l	290
	Thickness, h	204.66

III. SIMULATED RESULTS

In this section, the simulated and optimization result for base antenna and integration with buffer layer is presented. The optimization was done to get the optimum result to operate underwater. The result was analyzed in term of S_{11} and antenna efficiency.

A. Base Antenna Design

The base antenna design was simulated and optimized. Figure 4 represents the comparison in S_{11} results for the base antenna in normal condition and underwater. In normal condition, the base antenna was simulated in air environment setup while in underwater condition the base antenna was

simulated using distilled water background material. The results indicated that the base antenna in normal air environment setup yielded return loss S_{11}<-10 dB from 384 MHz to 1 GHz frequency band (and above), achieving wideband specifications, while in underwater conditions the antenna resonate at 250 MHz frequency band which is S_{11} = -14 dB. In term of gain and efficiency results the base antenna in air environment achieved gain = 2.29 dB and 93 % Efficiency, however the base antenna in underwater environment shows a poorer performances which is gain=-10.9 dB and 1.89 % Efficiency. Table IV presented the comparison on the base antenna performances operating in air and underwater environment.

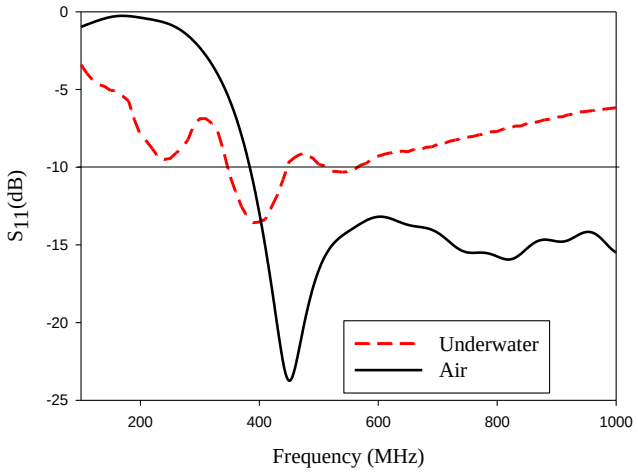

Fig.4. Comparison of base antenna performances in air and underwater environment

TABLE IV
COMPARISON BASE ANTENNA DESIGN PERFORMANCES OPERATING IN AIR AND UNDERWATER ENVIRONMENT

Antenna propagating Condition	Bandwidt/Resonate Frequency	Gain	Efficiency
Air Environment	>616 MHz/ 450 MHz	2.29 dB	93%
Underwater Environment	62 MHz/377 MHz	-10.9 dB	1.89%

B. Integration of Base Antenna with Buffer Layer Design

The performance of proposed antenna integrated with buffer layer structure was observed in term of S_{11}, gain and efficiency results. The results were observed with different buffer permittivity value (ε_{rb}) and different buffer size to achieve the optimum results. Figure 5 shows the simulated S_{11} result in four different ε_{rb} values and Figure 6 represents the S_{11} results for different size of buffer structure. From results in Figure 5, the antenna with buffer ε_{rb} = 8.85 shows the best S_{11} results which yielded S_{11} < -10 dB in wide frequency band which is from 450 MHz to 1 Ghz. The best S_{11} for buffer size is on reactive nearfield region buffer with consideration of buffer wavelength λ_b (h_4) which achieved wide frequency bandwidth S_{11} < -10 dB from 450 MHz up to 1 GHz.

The results on gain and efficiency were observed in three different resonating frequency. Figure 7 shows the three different frequency bands for each S_{11} with different permittivity value of buffer. The results was presented in Table V. Overall, the gain and efficiency performance for antenna with buffer ε_{rb} = 8.85 is better than the antenna without buffer and other permittivity value of buffer. It shows that the integration of buffer layer structure technique on the base antenna design produces a better results compared to the conventional base antenna design in underwater environment.

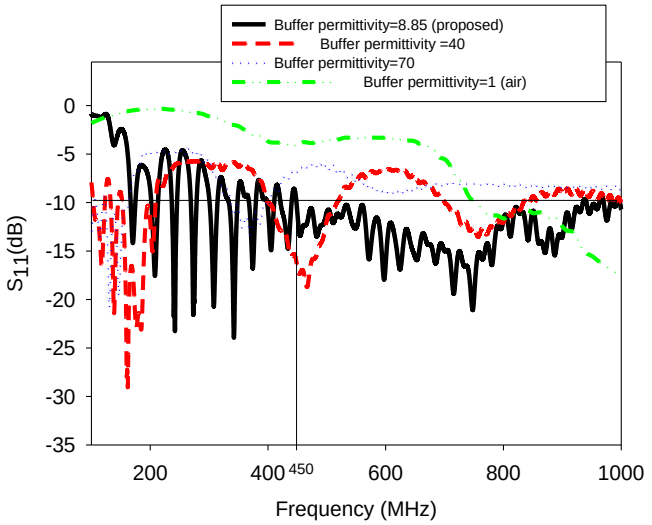

Fig.5. Simulated S_{11} result for antenna integrated with buffer layer structure with differences in ε_{rb} value

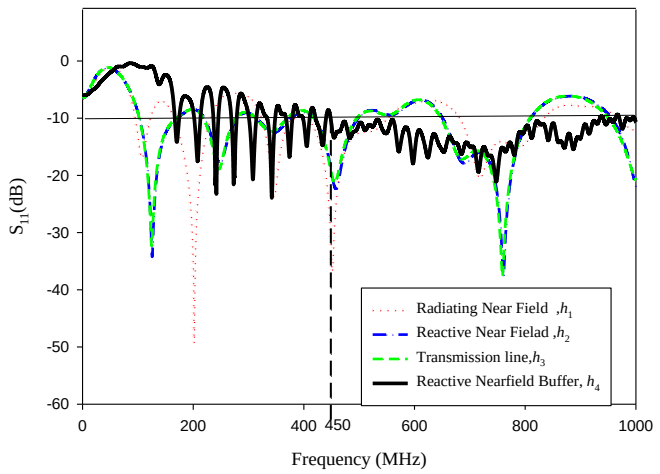

Fig.6. S_{11} results for different size of buffer structure.

TABLE V
GAIN AND EFFICIENCY RESULTS FOR ANTENNA WITH DIFFERENT PERMITTIVITY VALUE IN 3 FREQUENCY BAND

Band 1			
Antenna with buffer (ε_{rb}=8.85)	Bandwidth: 20 MHz Center freq: 435 MHz	Gain (dB) -4.93	% Efficiency 9.45%
Antenna without buffer	Bandwidth: 15 MHz Center freq: 238 MHz	Gain (dB): -3.67	% Efficiency 13.27%
Antenna with buffer (ε_{rb}=40)	Bandwidth: 56 MHz	Gain (dB): -6.78	% Efficiency 9.0%
Band 2			
Antenna with buffer (ε_{rb}=8.85)	Bandwidth: 81 MHz Center freq: 482 MHz	Gain (dB): -3.76	% Efficiency 10.0%
Antenna without buffer	Bandwidth: 61 Mhz Center freq: 377 Mhz	Gain (dB): -9.617	% Efficiency 2.49%
Antenna with buffer (ε_{rb}=40)	Bandwidth: 120 mhz Center freq: 467 MHz	Gain (dB): -10.2	% Effficiency 1.3%
Band 3			
Antenna with buffer (ε_{rb}=8.85)	Bandwidth: 396 Mhz Center freq: 748 MHz	Gain (dB): -4.88	% Efficiency 9.6%
Antenna without buffer	Bandwidth: 4 Mhz Center freq: 679 Mhz	Gain (dB): -12.43	% Efficiency 1.3%
Antenna with buffer (ε_{rb}=40)	Bandwidth: 139 Mhz Center freq: 752 MHz	Gain (dB): -13.2	% Efficiency 0.8%

IV. ACTUAL MEASUREMENT OF ANTENNA PERFORMANCE

In this section, the fabrication and experimental result for the base antenna and antenna with buffer layer will be presented. The antennas performances will be compared in term of S_{11}.

A. Measurement of Base Antenna Design

The base antenna design was fabricated and its performance was measured using a vector network analyzer while operating in air and underwater. The fabricated antenna dimensions is the same with the final simulated design. The performance of the base antenna in underwater was obtained by measuring the S_{11} when fully submerging the antenna inside a 230 × 110 cm water tank filled with tap water. Figure 8 presented the S_{11} measurement results for the base antenna in air and underwater environment.

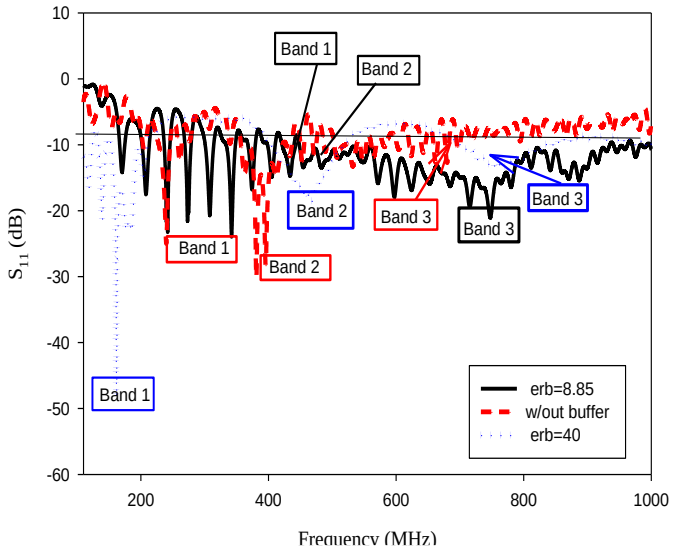

Fig.7. The three different frequency band for each S_{11} with different permittivity value of buffer.

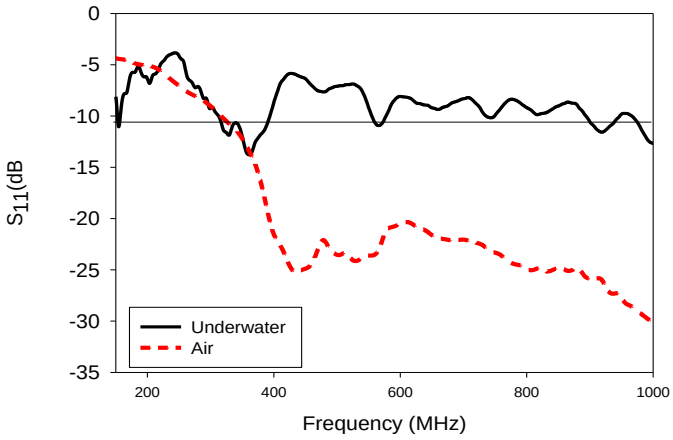

Fig.8. Comparison S_{11} measurement result for base antenna design in air and underwater measurement.

The results indicated that the base antenna S_{11} performance is very good in air environment which yielded S_{11} < -10 dB from 327 MHz to 1 GHz frequency band, indicating a wide frequency bandwidth within that frequency band. However, using the same base antenna in an underwater environment marked a significant reduction in the S_{11} performance. From the figure, it can be observed that the S_{11} is above the -10 dB line for almost all frequencies, except from 320 to 400 MHz. This reduction in performance is attributable to impedance mismatch since the antenna was designed at 50 ohm to match the impedance of air in atmosphere. However the propagation medium in underwater have different properties, hence resulting in impedance mismatch.

B. Base antenna integrated with Buffer Layer Structure.

The antenna integrated with buffer layer structure was fabricated and measured using similar setup as explained in Section IV(A). The fabricated antenna and the measurement scenario are shown in Fig. 9. A new liquid properties were proposed as a material for buffer layer design. In this study, liquid was chosen as the buffer material because it is relatively easy to synthesize and apply parameter tuning. The best solution that produces ε_{rb} nearest with 8.85 is methyl acetate (CH_3COOCH_3) with ε_{rb} = 6.65. To produce a liquid solution with ε_{rb} similar to the simulated value (ε_{rb} = 8.85), the solution was diluted using distilled water. Figure 10 shows the measured relative permitiitivy values of different ratios of distilled water and methyl acetate. It was found that the mixture of methyl-acetate (1 mol/l) and distilled water with ratio 7:1 produced the nearest value as the simulated ε_{rb}. This recipe was used as the buffer layer material (termed "optimized buffer layer") in all of the measurement results presented afterwards. Figure 11 shows the antenna S_{11} measurement results comparing three different conditions which are; without buffer, with buffer containing air, and with the optimized buffer layer (ε_{rb} = 8.85). From the figure, it was observed that the antenna with the optimized buffer produced the best performance among the three cases, marking return loss below -10 dB from 20 to 400 MHz and 450 to 1 GHz.

Figure 12 presented a comparison between simulated and measured of S_{11} of antenna with the optimized buffer layer. It can be observed that the measurement shows similar trend of S_{11} curve as the simulated result, proving the proposed antenna ability to operate well underwater. There is however some slight discrepancies where the simulated S_{11} curve marked multiple nulls and worse S_{11} in the lower frequencies (below 400 MHz). These discrepancies is attributable to the antenna fabrications errors and external factor from measurement environment such as unaccounted surface current and reflections from enclosed water tank walls, which affected the measured result. However, the measured results were deemed sufficient to reproduce the trend obtained by the simulated results.

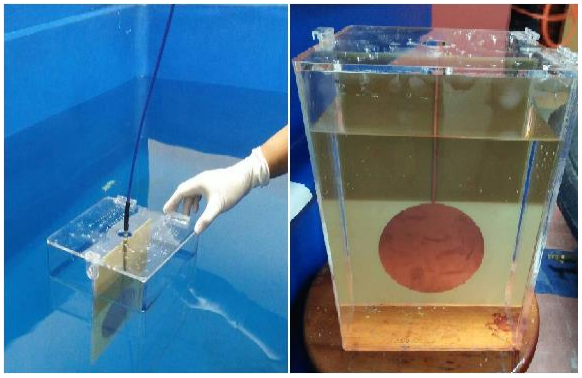

Fig.9. Measurement setup for S_{11}

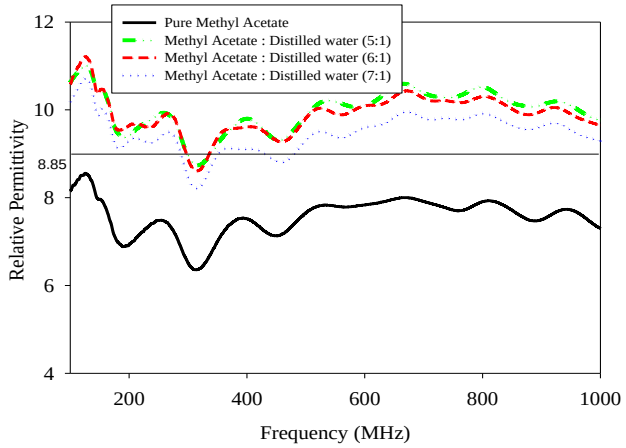

Fig.10. Optimization on buffer relative permittivity (ε_{rb}) of a mixture methyl acetate and distilled water

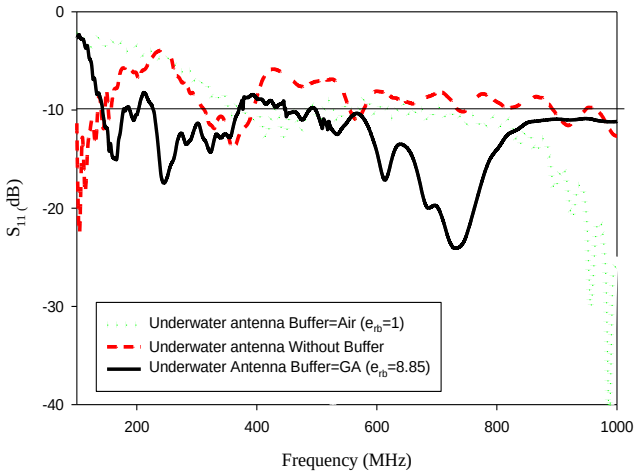

Fig.11. Measured S_{11} result for antenna integrated with buffer layer structure with differences conditions.

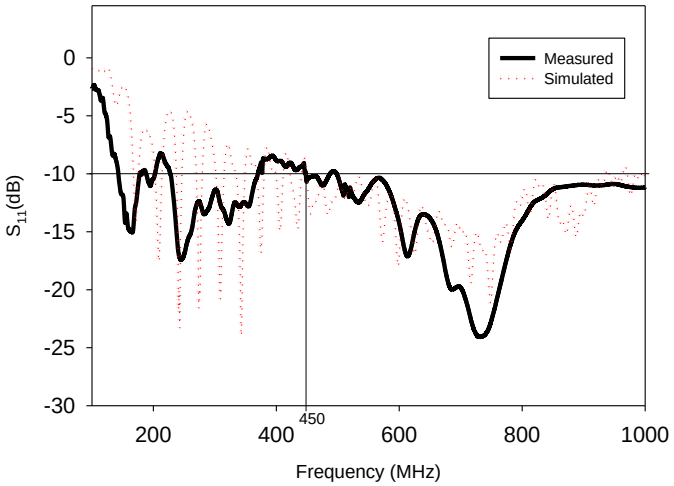

Fig.12. Comparison between simulation and measurement of S_{11} of antenna with optimized buffer layer

V. CONCLUSION

This paper presents a wideband circular patch antenna with an optimized buffer layer structure for underwater application. The buffer layer was developed using a liquid material which have a relative permittivity (ε_{rb}) of 8.85, equals to the geometric average value between the permitivitty of air and water. A solution consists of a mixture of methyl acetate and distilled water with 7:1 ratio was used as the buffer recipe. The buffer size was set to be similar to the reactive nearfield region of the antenna. Based on a series of simulation and actual measurements in laboratory setup, it was shown that the the proposed antenna design with an optimized buffer layer permittivity and size resulted in an improved antenna performance compared to conventional insulated antennas, when operating underwater within the desired frequency. Future works will include multi-layer buffer designs, and application to underwater propagation measurements.

ACKNOWLEDGMENT

The authors would like to acknowledge Ministry of Higher Education (MOHE) of Malaysia for providing the funds that supported the research presented in this paper, through the Fundamental Research Grant Scheme (FRGS), grant no. 600-RMI/FRGS 5/3 (39/2015).

REFERENCES

[1] T. P. Sameer Babu and S. S. Kumar, "Underwater Communications," in IEEE Underwater Technology, pp. 1-3, 2015.

[2] E. A. Karagianni, "Electromagnetic waves under sea: Bow-tie antenna design," Progress in Electromagnetic Research M, vol. 41, pp. 189-198, 2015.

[3] P. A. Van Walree, and R. Otnes, "Ultrawideband Underwater acoustic communication channels," IEEE Journal Of Oceanic Engineering, vol. 38, No. 4, 2013.

[4] G. Hattab, M. El-Tarhuni, T. Joudeh and N. Qaddoumi, "An underwater wireless sensor network with realistic radio frequency path loss model," Int. Journal of Distrubuted Sensor Network, vol. 9, Article ID 508708, 2013.

[5] H. D. Trung and V. D. Nguyen, "An analysis of mimo-ofdm for underwater communications," in Ultra Modern Telecommunications and Control Systems and Workshops, pp. 1–5, 2011.

[6] B. Kelley, K. Manoj, and M. Jamshidi, "Broadband RF communications in underwater environments using multi-carrier modulation," in IEEE Int. Conf. on Systems, Man and Cybernetics, pp. 2303–2308, 2009.

[7] H. Fabian, G. Mendez, G. A. C. Christian, et al, "High Performance Underwater UHF Radio Antenna Development," in IEEE OCEANS 2011, pp 1-5, 2011.

[8] E. Telecomunicacion, E. Jimenez, G. Quintana, P. Mena, P. Dorta, I. Perez-alvarez, S. Zazo, and M. Perez, "Investigation on Radio Wave Propagation in Shallow Seawater : Simulations and Measurements," IEEE Third Underwater Communications and Networking Conference (UComms) pp. 1–4, 2016.

[9] H. Yoshida, N. Iwakiri, T. Fukuda, M. Deguchi and S. Onogi, "Measurements of underwater electromagnetic wave propagation," in 2015 IEEE Underwater Technology, pp. 1-5, 2015.

[10] H.Yoshida, N.Iwakiri, T.Fukuda , M. Deguchi ans S. Onogi, "Measurements of underwater electromagnetic wave propagation, 2015 IEEE Underwater Technology, pp.1-5,2015

[11] V. T. Nguyen and C. W. Jung, "Impact of dielectric constant on embedded antenna efficiency, " Int. Journal of Antennas and Propagation, vol. 2014, Article ID 758139, 2014.

[12] I. Pasya, H. M. Zali, M. Saat, and M. T. Ali, T. Kobayashi," "Buffer Layer Configuration for Wideband Microstrip Patch Antenna for Underwater Applications", Loughborough Antennas & Propagation Conference (LAPC),pp. 1 - 5, 2016.

[13] Islam Md. Rafiqul, Alam AHM Zahirul, M. Feroze Akbar J. Khan and Shaker Alkaraki, " Design of Microstrip Patch Antenna Using Slotted Partial Ground And Addition Of Stairs And Stubs For UWB Application" Multidisciplinary Journals in Science and Technology, Journal of Selected Areas in Telecommunications (JSAT), May Edition, 2012.